JOURNAL OF Materials CHEMISTRY

Hexamethyldisiloxane (HMDSO)-plasma-polymerised coatings as primer for iron corrosion protection: influence of RF bias

Christine Vautrin-Ul,*[a] Françoise Roux,[a] Caroline Boisse-Laporte,[b] Jean Louis Pastol[c] and Annie Chausse[a]

[a]*Laboratoire Analyse et Environnement, UMR 85 87, C.N.R.S-C.E.A-Université d'Evry Val d'Essonne, 1 Rue du Père Jarland, 91 025 Evry, France. E-mail: christine.vautrin-ul@chimie.univ-evry.fr*
[b]*Laboratoire de Physique des Gaz et des Plasmas, UMR 85 78 Bat. 210, C.N.R.S-Université Paris Sud 91 405 Orsay Cedex, France*
[c]*Centre d'Etudes et de Chimie Métallurgique, UPR 2801, C.N.R.S, 15 rue Georges Urbain, 94 407 Vitry sur Seine Cedex, France*

Received 17th December 2001, Accepted 9th May 2002
First published as an Advance Article on the web 20th June 2002

Silicone-like coatings were prepared by plasma enhanced chemical vapor deposition on steel substrates using a hexamethyldisiloxane–oxygen (80 : 20) precursor mixture, in a microwave reactor. The plasma composition, the structure and barrier properties of the coatings were studied as a function of the RF bias. OES was carried out in order to identify the excited species in the plasma. The coatings were characterized by several *ex situ* diagnostics including FTIR, SEM, gravimetry and EIS.

OES, using argon as an actinometer, showed no modification in the HMDSO dissociation as the RF bias varies; but it indicated changes in the chemical recombination reactions. Coating analyses revealed that radio frequency (RF) bias induced a densification of the coatings associated with modifications in their morphology and chemical composition. Results were explained using the general mechanism in the literature relative to plasma-deposited thin films. EIS results indicated that the best barrier properties during immersion in NaCl solutions were obtained with coatings deposited under high RF bias.

1. Introduction

The most convenient method for preventing the corrosion of metals is the application of protective organic coatings because they have two main features, good adhesion to the metal substrate and corrosion protection.[1] Protective properties are provided generally by both the surface pretreatment including conversion layer and the primer. Surface/primer treatments currently used to improve adhesion and to provide metal corrosion protection are based on toxic and environmentally hazardous materials such as chromate or phosphate. Recently, much interest has been focused on developing a non-toxic replacement.[2,3] Several alternative primer systems have been studied such as electrodeposited coatings,[3] conducting polymer coatings,[4] sol–gel coatings[5] and plasma polymer coatings.[6]

Plasma deposition is an environmentally friendly process used to create ultrathin good quality coatings on substrates at low temperatures. Plasma coatings have two invaluable properties as primer coatings for corrosion protection: a highly cross-linked matrix and covalent bonds between the substrate and the coating. Thus the coatings display a very good chemical resistance and an excellent adhesion. A combination of substrate cleaning, pretreatment and polymer deposition steps is possible during the process[6,7] thereby avoiding the risk of contamination of the surface. The use of Si-containing monomer precursors leads to coatings which show better corrosion protection than hydrocarbon or fluorocarbon plasma-coatings. Among Si-containing precursors, the most used are tetramethylsilane (TMS), tetraethoxysilane (TEOS) or hexamethyldisiloxane (HMDSO). Both TEOS and HMDSO are non-toxic, non-explosive and much safer than TMS. HMDSO has the further advantage of a higher room temperature vapor pressure than TEOS which allows easier use.[8]

Plasma deposition of silicone-like coatings has been widely investigated for applications in semiconductor technology and in food packaging.[9–13] Depositions were also done on metal substrates for applications in metal corrosion protection.[14–19] It is well known that the coatings strongly depend on the deposition process parameters. For example, either inorganic SiO_2-like coatings or silicone-like coatings are deposited according to the HMDSO : O_2 ratio. In some of our previous works,[14,15] we correlated the nature of the coatings with their barrier properties against iron corrosion in NaCl solutions. Silicone-like coatings present good anticorrosion performances and the best protection is obtained when the HMDSO content in the precursor mixture reaches 80%.

Loss of barrier properties results from the presence of a number of tiny defects (pinholes) in the silicone-like coating in which the electrolyte diffuses as far as the iron surface. This loss is obtained even if the major part of the iron surface is covered with a well-adhering, impermeable coating.[15] Application of an RF bias to the substrate affects the energy of the impinging ions so that it allows control over the ion energy during the coating growth.[20] At high bias values, ions have high energy and play a role not only in the surface processes but also in the composition and the microstructure of the coatings (number of pinholes).[21]

In this work, we study the influence of the RF bias on the excited species in the plasma, on the structure and the corrosion protection properties of coatings deposited on iron samples using a HMDSO–O_2 (80 : 20) precursor mixture. The excited species are identified by optical emission spectroscopy (OES). The coatings are characterized by infra-red spectroscopy (IR spectroscopy), scanning electron microscopy (SEM) and gravimetry; corrosion properties are estimated by electrochemical impedance spectroscopy (EIS).

 DOI: 10.1039/b111509j

2. Experimental

2.1. Coating deposition

The experimental apparatus has been presented in detail elsewhere.[14,22] A plasma is generated using a Surfaguide Reactor Excitator[23] fed from opposite sides by two microwave (MW) sources at 2.45 GHz; each of them is set typically at 700 W of power. Plasma is produced in a quartz tube (inner diameter 12 cm, length 40 cm) which ends in a cylindrical chamber (inner diameter and length are 50 cm) containing a substrate holder. The gases (dioxygen O_2 and argon Ar) are injected at the top of the MW discharge tube. Argon is added as a reference gas for emission spectroscopy measurements. Hexamethyldisiloxane, HMDSO (Sigma, Aldrich) is heated at 40 °C and is injected into the diffusion chamber *via* a ring with 20 pierced holes. This ring is set 5 cm under the MW discharge tube and 10 cm above the vertical substrate holder which can support 6 samples (iron disks 1.5 cm in diameter and 1 mm in thickness). Radio frequency (RF) power can be applied to the substrate holder. The maximum used power is 160 W at 13.56 MHz. The effects of the RF power are biasing and creation of a plasma around the substrate. The flows of gases and HMDSO are controlled by mass flowmeters and are given in standard centimetre cube units (sccm). The flows have been set typically as follow: O_2 12 sccm, HMDSO 45 sccm and Ar 4 sccm. The total pressure is about 40 mTorr.

The deposition procedure is as follows. First, iron disks (Goodfellow, purity 99.5%) are polished and before deposition are treated in the MW reactor without RF bias with oxygen plasma (150 sccm) for 10 minutes. Afterwards, the coating process proceeds with MW and RF powers using the typical conditions stated above. The duration of coating deposition varies from 6 minutes to 20 minutes to obtain the desired thickness of coatings about 1 μm. Finally, after deposition, MW and RF powers are turned off; the iron disks are left in the reactor for 15 minutes in an argon flow (900 sccm) for cooling.

The phase gas was characterised by means of optical emission spectroscopy that allows the detection of the excited species in the plasma near the samples. The plasma emission was collected with an optical fibre located in the chamber near the substrate. The fiber was equipped with a collimator, which prevented the observation of more intense emission from microwave discharge. The signal was analysed in the 200–850 nm range using a monochromator HR460 Jobin & Yvon equipped with a CCD detector (1024 × 256 pixels).

2.2. Coating analyses

The coating structure was analysed by means of reflection absorption IR (RAIR) measurements performed using a Brüker IFS28 spectrometer controlled by a Compaq computer using the Opus software. The spectra of the plasma-polymerised coatings were typically obtained by averaging 20 scans and then subtracting the spectrum obtained from the substrate before deposition of the film.

The coating density was measured by gravimetry. The coating thickness was measured with a profilometer (Dektak 3030, Sloan). The iron samples were weighed before and after coating with a micro-scale balance (Sartorius MC210). The density of the coatings was determined from the weight increase to the thickness ratio. The surface morphology of the plasma-polymerized coatings was studied using a LEO 1530 Field Effect Gun Scanning Electron Microscope (FEG-SEM). This apparatus provides high resolution secondary electron images even for low electron beam energies. For better imaging of the surface, the samples were covered with a 2 nm layer of Pt–Pd alloy, then observed using an 1 keV electron beam.

The corrosion protection of the coatings was analysed by means of electrochemical impedance spectroscopy (EIS) measurements. EIS data were obtained using a Schlumberger Solartron 1255 frequency response analyser coupled to an EGG PAR 273 potentiostat/galvanostat. Impedance data were collected at frequencies ranging from 10 mHz to 100 kHz. Typically measurements were made at 5 points per decade, 10 mV ac amplitude. An electrochemical cell with three electrodes was used. Coated iron sample were used as working electrode (area 0.8 cm^2) and a platinum grille served as counter electrode. A saturated calomel reference electrode was employed. The experiments were conducted at room temperature with NaCl 0.1 mol L^{-1}.

3. Results

3.1. Plasma chemical characterisation

Optical emission spectroscopy (OES) samples the plasma emission of electronically excited species; it allows deduction of semi-quantitative trends of emitting species as a function of an experimental variable, the RF bias in this work. 6% argon, a non-reactive gas, was added to the HMDSO–O_2 precursor mixture in order to perform semi-quantitative analysis (actinometric optical emission spectroscopy or AOES).

Fig. 1 reports the emission intensity of different species which were detected during this study as a function of the RF bias, at a given microwave power (700 W on each side): Ar (811 nm) line (Fig. 1a) and O (844 nm), Hα (656 nm), CH (431 nm), C_2 (516 nm), CO (519 nm) lines (Fig. 1b). The argon line increases linearly with increasing RF bias. This increase relative to a non-reactive gas may be attributed, according to the literature, to an increase of both the local plasma density around the substrate and electron temperature. Lines of all the other species derived from the HMDSO–O_2 mixture also increase with the RF bias. Interpretation here is difficult because emission lines are related to the upper excited state of species; different origins are possible to justify this increase: increase of the species in its fundamental state, increase of the plasma density and electron temperature. In order to avoid the influence of the plasma density and electron temperature, an actinometric approach was used so that the density of species X in the ground state can be considered proportional to the emission intensity of X itself divided by that of argon.[24] This supposes that three conditions are satisfied: (i) the excitation process of species X is a direct electron collision, (ii) the loss of the upper level of the emission intensity of X is a radiative process, (iii) the excitation cross sections of the upper levels of

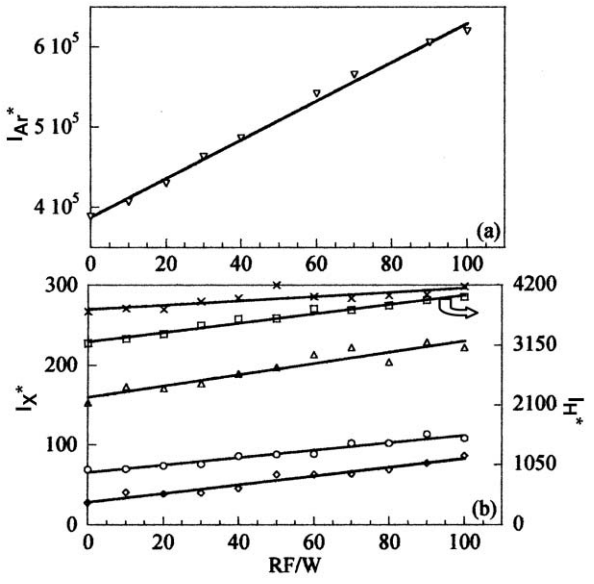

Fig. 1 (a) Emission intensity of Ar (811 nm) line *vs.* the RF bias. (b) Emission intensity lines *vs.* the RF bias: O (844 nm): (Δ) ; Hα (656 nm): (□) ; CH (431 nm): (○) ; C_2 (516 nm): (×) ; CO (519 nm): (◊).

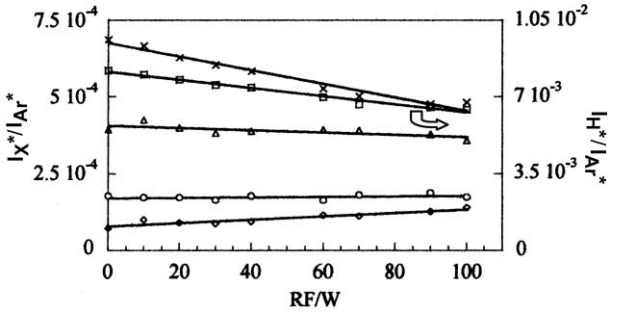

Fig. 2 Normalized emission intensity lines *vs.* the RF bias of O (844 nm): (Δ); Hα (656 nm): (□); CH (431 nm): (○); C_2 (516 nm): (×); CO (519 nm): (◊).

I_{ar} and I_x have excitation thresholds of the same order and the same behaviours with electron energy. These assumptions can be rather speculative for some species, such as H atoms where chemical excitation channels are also possible[25] and molecules and radicals where the excitation thresholds (a few eV) are far from that of the actinometer (15 eV).

Results of the actinometric approach are given in Fig. 2. No obvious influence of the RF bias on the normalized emission intensities of O and CH species is obtained; so we can conclude that the HMDSO molecule dissociation is constant when the RF bias increases. This result is consistent with literature data which indicate that the precursor dissociation in the gas phase is mainly controlled by the microwave power.[26] Consistent with this, our results indicate a modification of normalized emission lines of species which result from chemical recombination reactions of atoms composing HMDSO (decrease of emission line of C_2 species) or recombination reactions with the oxygen from the plasma (increase of emission line of CO species). CO species are given in the literature as indicative of etching products during deposition such as CO, CO_2 or H_2O.[27] The normalized emission line of H decreases with the RF bias but interpretation here is difficult because of the possible occurrence of chemical excitation channels as stated above.

Note that our conclusions concern the species detected in this work but we have no information on high molecular weight fragments of HMDSO or on Si species (SiO 252 nm and Si 288 nm), which are not detected because of their low emissivity or their low content.

3.2. Coating characterisation

3.2.1. Gravimetry measurements. The influence of the RF bias on the deposition rate is measured by gravimetry and is reported in Fig. 3. With increasing RF bias, the deposition rate increases until it reaches the level of 140 nm min^{-1} or 40 μg min^{-1} and then remains nearly constant. As the weight increase (×13) exceeds the thickness increase (×7), the coating density changes; it ranges between 0.9 and 1.6 g cm^{-3} as the RF bias increases from 0 to 120 W.

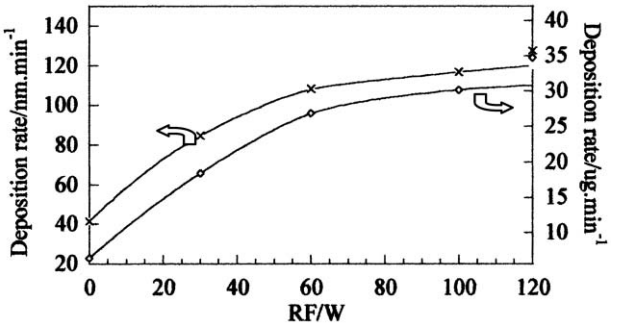

Fig. 3 Deposition rate *vs.* the RF bias: (×) nm min^{-1} or (◊) μg min^{-1}.

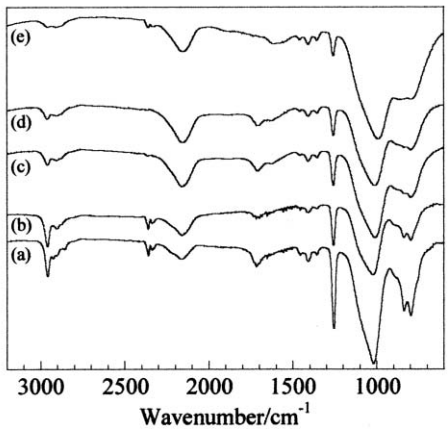

Fig. 4 FTIR spectra relative to plasma-polymerized coatings on iron substrates *vs.* the RF bias: (a) 0 W; (b) 30 W; (c) 60 W; (d) 100 W; (e) 120 W.

It is well known that HMDSO coatings deposited in oxygen-rich mixtures have a density close to that of the thermal oxide SiO_2 (2.2 g cm^{-3}). When the deposition is done in HMDSO-rich mixtures, the coating density decreases and approaches generally a value around 1.4 g cm^{-3}.[14,27] The difference in densities is attributed to changes in inorganic/organic features of the coatings. Further data in the literature also indicate that the RF bias induces a coating densification by the limitation of voids in the porous structure.[21] So, interpretation of gravimetry results is difficult and FTIR measurements were done in order to attribute the density increase either to a chemical modification or to a physical modification, both induced by the RF bias.

3.2.2. FTIR measurements. Reflexion absorption infrared spectroscopy (RAIR spectroscopy) was used to follow changes in the bonds of coatings. The evolutions of the infrared spectra with RF bias are shown in Fig. 4; the infrared bands are assigned according to the literature.[28,29] The main vibrational modes of the monomer (HMDSO) were found in the plasma-polymerised coatings: the two CH_3 stretching modes at 2850 and 2950 cm^{-1}, the deformation mode of $(CH)_X$ at 1400–1430 cm^{-1}, the CH_3 rocking in $Si(CH_3)_X$ at 1260 cm^{-1}, the Si–O asymmetric stretching in the region around 1000 cm^{-1}. The following bands can be noted elsewhere: a broad band centered at 2115 cm^{-1} is consistent with the region of the Si–H stretching mode, a weak band at 1710 cm^{-1} corresponding to the C=O groups, and a weak peak at 1350 cm^{-1} assigned to the $–CH_2$ scissoring and wagging vibrations in $Si–CH_2–Si$.

The increase of RF bias leads to (i) a shift of the Si–O stretching (1060 to 1040 cm^{-1}), (ii) an increase of the intensity of Si–H stretching peak (2115 cm^{-1}) and (iii) a decrease of the intensity of the bands due to the carbon bonds ($–CH_3$ at 3000 cm^{-1}, $Si–CH_3$ at 1240 cm^{-1} and C=O at 1710 cm^{-1}). The shift of Si–O to lower values is reported in the literature to be the consequence of a microscopic densification of the materials;[30,31] but it can also result from the creation of Si–H. In order to validate this, we report the increase of the relative Si–H intensities as a function of the coating density (Fig. 5). A correlation is effectively obtained between the relative Si–H intensities and the density. At the same time, Fig. 5 clearly shows a decrease of the relative $Si–CH_3$ intensities with the coating density. So, we can assume that the increase of RF bias changes the plasma-polymerised coating's structure with a loss of carbon; the plasma-polymerised coatings tend to be less organic with an increase in RF bias, as already reported in the literature.[27]

3.2.3. SEM analyses. An example of a scanning electron micrograph (SEM) of HMDSO plasma-polymerised coatings is

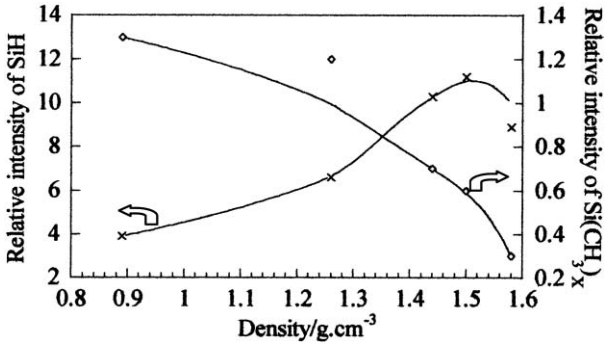

Fig. 5 Evolution of the normalized absorbance as a function of the coating density: (×) Si–H band (2100–2250 cm^{-1}); (◊) Si–CH_3 band (1260 cm^{-1}).

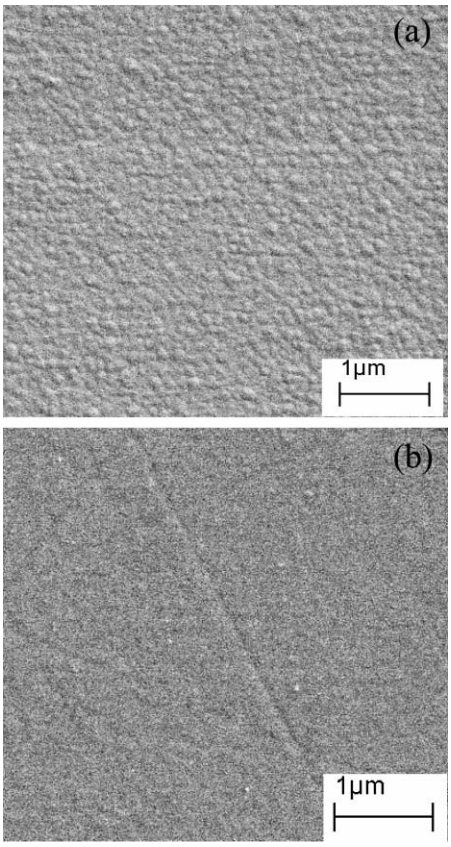

Fig. 6 SEM micrographs of plasma-polymerized coatings obtained at RF bias: (a) 0 W and (b) 100 W.

shown in Fig. 6. All the samples show a uniform surface of the coatings with few defects such as protuberances or pinholes. However the surface morphology is strongly affected by the RF bias. The coatings shown in Fig. 7 were obtained at different RF bias, respectively 0 W and 100 W. The pictures relative to plasma-polymerised coating at RF bias 0 W present clear grain boundaries of irregular shapes. The grain size is around 300–500 nm in length and 200 to 300 nm in breadth. Within each aggregate, there are a collection of spherical grains with an average diameter of approximately 20 nm (Fig. 8). For coating deposited at RF bias 100 W, the grain size is smaller, around 100 nm in length and in breadth. The grain size decreases significantly as the RF bias increases. The grain boundaries are less distinct in the coating obtained at RF bias above 50 W and their surface seems to be smoothed. In conclusion, SEM analyses suggest that the RF bias has an influence on the coating morphology.

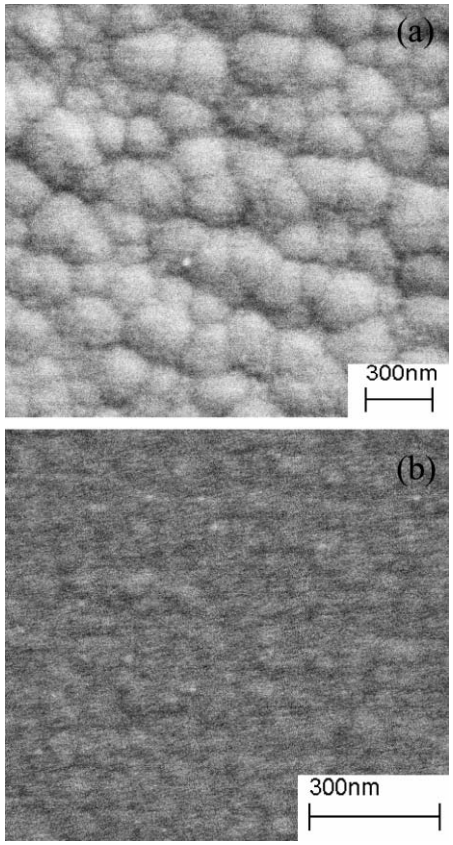

Fig. 7 SEM micrographs of plasma-polymerized coatings obtained at RF bias: (a) 0 W and (b) 100 W.

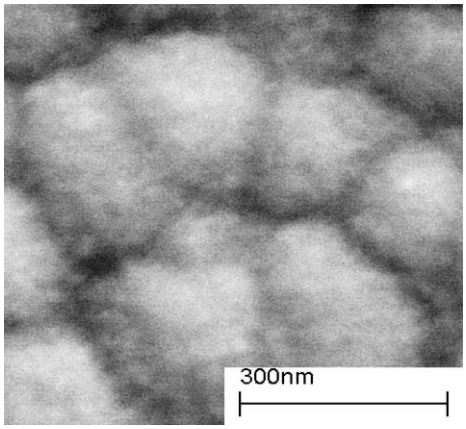

Fig. 8 SEM micrograph of plasma-polymerized coating obtained at RF bias 0 W.

3.3. Corrosion protection properties of the coatings

The process of corrosion depends upon several parameters, namely the diffusion of water, ions and oxygen through the coating, the adhesion between metal substrate and coating and the rate of adhesion loss. Surface cleaning and pretreatments were an important step to improve adhesion. An advantage of the plasma techniques is the possibility of pretreatment and cleaning of the metal surface. Under plasma conditions, it is easy to clean the surface before the polymer coating deposition without exposing the substrate surface to air. With a non-polymer forming gas such as N_2, O_2, Ar, H_2 *etc.*, plasma treatments can be used to clean and to modify the metal surface without altering the bulk properties. This process can be used in the preparation of the metal surface and thereby allows improvement of the adhesion of the plasma polymer coating. According to our preliminary studies, we have chosen an O_2

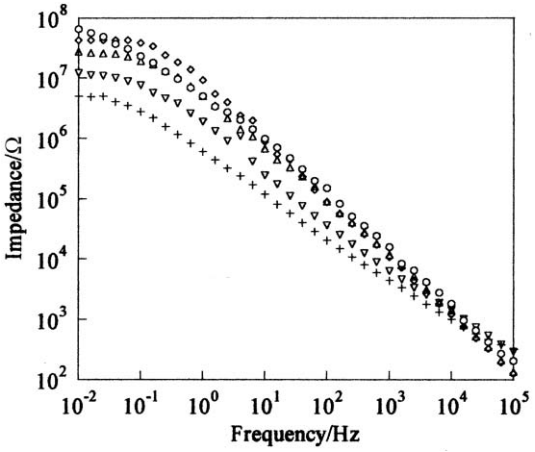

Fig. 9 EIS spectra of plasma-polymerised coatings on iron substrate deposited at various RF bias at initial immersion time in NaCl solution: (+) 0 W; (∇) 30 W; (Δ) 60 W; (◊) 100 W; (○) 120 W.

pretreatment steel surface which is recognized to improve the corrosion protection properties in the case of a HMDSO plasma polymer coating.[32]

Electrochemical impedance spectroscopy (EIS) has already been used to predict the life of organic coatings used for corrosion protection. The technique is based on the measurement of the current response on small sinusoidal perturbations of the electrode potential as a function of the frequency of the perturbation. EIS has proven to be a powerful tool to rapidly obtain system specific parameters of coatings, especially for evaluating the early deviation of organic coatings from their initial capacitive behaviour.[33] In Fig. 9, typical Bode plots of HMDSO plasma polymerised coatings, deposited on iron at several different RF bias values after 10 minutes of immersion in NaCl solutions, are given. All the coatings have the same thickness (0.8 $\pm$0.1 μm). These plots were analysed to determine the total capacitance C_t and the total resistance R_t.[34] The total capacitance of these systems can be determined by extrapolation of the impedance *vs.* frequency curves in the 10^1 to 10^3 Hz range to intercept the impedance axis at 0.16 Hz according to the model proposed by Mansfeld.[35] The total resistance can also be determined from the intercept of the horizontal portion of the same curve in the low frequency range (10^{-2} to 10^0 Hz).[35] The values of C_t and R_t are reported in Table 1. The total capacitance corresponds to the dielectric response on the coating and can provide information on the solution uptake, since the incorporation of molecules in the coating leads to an increase in the relative permittivity of the film and thereby an increase of C_t. R_t represents in fact the corrosion resistance[36] which is the sum of all the resistances: the pore resistance, the polarization resistance and the electrolyte resistance.[34] Although this type of analysis is qualitative, it allows the establishment of a ranking order of the different deposited films. The values of the total capacitance and the total resistance are close to 10 nF and 10^7 Ω respectively. One may notice the slight increase of R_t and decrease of C_t with the RF bias increase. One may conclude that all the coatings have approximately the same behaviour at initial immersion time with a best protection for the coating obtained at RF bias superior to 60 W. Those Bode plots are indicative of only one distinct RC circuit, that of the porous coating.

Table 1 Summary of electrochemical impedance spectroscopy results of plasma-polymerised coatings, from different RF bias, deposited on iron samples at initial immersion time

RF/W	0	30	60	100	120
$C_t/10^{-8}$ F	43.5	12.7	3.8	2.3	4.3
$R_t/10^7$ Ω	0.52	1.3	6.5	4.5	2.8

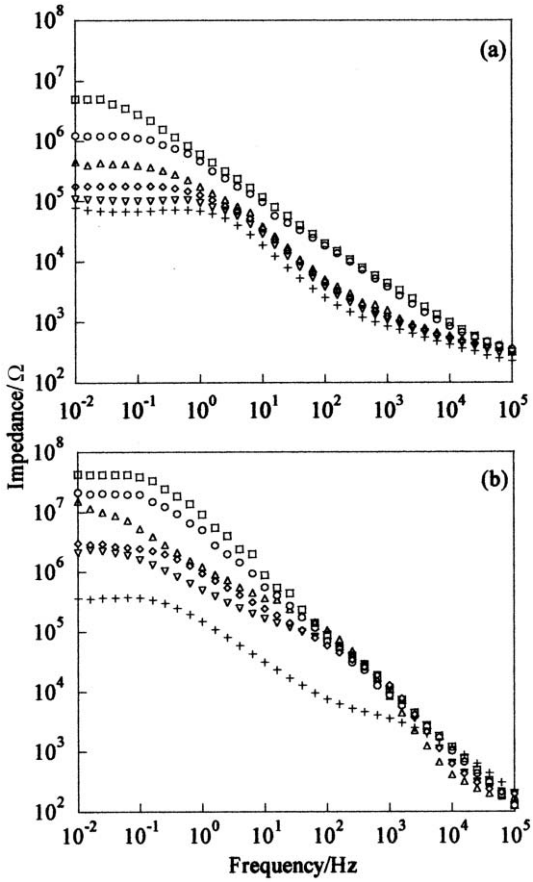

Fig. 10 (a) EIS spectra relative to plasma-polymerised coatings deposited on iron substrate at 0 W RF bias: (□) 0; (○) 8; (Δ) 24; (◊) 72; (∇) 120; (+) 192 hours of immersion in NaCl solutions. (b) EIS spectra relative to plasma-polymerised coatings deposited on iron substrate at 100 W RF bias: (□) 0; (○) 8; (Δ) 72; (◊) 120; (∇) 192; (+) 360 hours of immersion in NaCl solutions.

EIS Bode plots at different immersion times are shown in Fig. 10a and 10b for the coatings obtained at 0 W and 100 W respectively. For all the samples, a general pattern of behaviour can be drawn. Different steps are observed corresponding to the initiation and the propagation of the corrosion on iron coated disks.

The impedance values in the low frequency region decrease as a function of immersion time. This first step is due to the swelling and ion incorporation of the plasma-polymerised coatings. This first step is that much longer since the RF bias is high: 30 hours for the coating obtained at 100 W and less than 8 hours for the coating obtained at 0 W.

In a second step, for longer immersion times, the shapes of the EIS Bode plots are modified and correspond to the microscopic delamination of the coatings. The decline of the impedance values at low frequencies is a function of immersion time and is slightly more for high RF bias coating (60 to 120 W). The influence of the RF bias seems to control the rate of the decline. One may conclude that the coatings deposited with high RF bias have the best barrier properties and the best behaviour when the exposure time increases. This fact could be explained on one hand by the higher density of the plasma-polymerised coatings, and, on the other hand, by the highest homogeneity of the coatings observed by means of SEM.

4. Discussion

This work was devoted to the influence of the RF bias on the structure and properties of coatings deposited on iron

substrates from HMDSO–O_2 (80 : 20) precursor mixture. Applying a RF voltage to the substrate induces a negative bias voltage to the substrate holder. Ion bombardment of the growing coating during deposition induces changes in chemical and physical properties and consequently changes in structural morphologies of the deposited films.

During the coating process, AOES was used to identify the plasma species and to deduce semi-quantitative trends of emitting species as a function of the RF bias. The RF bias has no influence on the normalized emitting lines of O and CH species; this indicates, in accordance with literature data, that HMDSO precursor dissociation is mainly controlled by the microwave power. But recombination reactions are affected by the RF bias. A correlation can be made between C_2 and CO emitting species that derived from recombination reactions; a factor of 2 is found between the decrease of the normalized emitting intensity of C_2 and the increase of the normalized emitting intensity of CO. This suggests that C_2 species are redissociated in the plasma as the RF bias increases; C is consumed in CO formation. The invariance of the normalized emission line of O is explained as a result of a balance between oxygen dissociation and oxygen consumption in CO formation. So, we can suppose that the increase of the electron density *via* the RF bias enhances the oxygen dissociation, but it does not change the dissociation of HMDSO due to its strong SiO bonds.[37] No Si species (either high molecular weight fragments of HMDSO or SiO, Si–H and Si) were detected in the plasma using AOES so that we can not confirm this possibility.

FTIR on coatings were done to follow changes in the bonds with increasing bias. Results show a decrease of the intensity of the carbon bonds and an increase of the Si–H bonds. Such SiH stretching mode has been already detected by infrared absorption of plasma and was attributed to Si–H in a big fragment RSi–H of the HMDSO parent molecule.[37] Attempts of correlations between the species in the plasma and the chemical composition of the coatings failed here because of the lack of information on Si species. However, the presence of big fragments of the HMDSO parent molecule is consistent with the partial dissociation of HMDSO already discussed above. Note that the Si–H bonds do not exist in the HMDSO precursor and they could result from the adsorption of H radicals or other H species during the coating growth. FTIR analyses also indicate a decrease of the carbon bonds in the coatings with increasing RF bias. This can be correlated with the enhancement of oxygen dissociation by the RF bias stated above; the resulting oxygen species have an etching effect on the carbon so that the coatings are less rich in carbon. However, with regard to the HMDSO–O_2 (80 : 20) mixture, we can suppose that the oxygen atom flux at the surface of the growing coating is too weak to prevent all carbon incorporation into the coating even at high RF bias.

The creation of Si–H bonds induces a densification of the coatings that is also revealed by gravimetry. Gravimetry also indicates a rate increase with the RF bias. This is consistent with the evolution of CO emission intensity. This last one is directly linked to the coating growth kinetics assuming that CO is mainly created either from the ground state radicals or by dissociation of CO_2; all these species are generated by surface reactions.[38]

SEM analyses show the influence of the RF bias on the coating morphology. Results will be explained using the general deposition mechanism for plasma deposited thin films proposed by Favia *et al.*[39] In a first step, precursors undergo, *via* electron impacts, a fragmentation into inorganic and organic fragments; in a second step, these fragments can be adsorbed on the substrate surface. This adsorption is greatly influenced by the RF bias. As a negative voltage is applied to the substrate holder positive ions can hit the growing coating. These ions can create active sites at the surface (low-energy ions), depress precursor adsorption and/or trigger etching processes (high-energy ions). As the grain size significantly decreases with increasing the RF bias, we can suppose that the number of active sites increases and that positive ions hitting the growing coating are low-energy ions. The deposition rate is consistent with this conclusion, as it increases with the RF bias. Indeed, this increase implies that the etching process plays a minor role because the deposition rate is the result of a balance between etching and the growth mechanism of the coatings.

The surface roughness can result from the creation of active sites but it can also arise from other phenomena. Firstly, the literature reports that very smooth coatings can be obtained when impinging species have enough energy to bond at their first contact point.[40] This could be done by the second plasma around the substrate holder that allows control over the ion energy during the coating growth. Secondly, applying a negative voltage to the substrate holder can enhance the role of positive ions in the growth mechanism with regard to radicals or neutral species; positive ions can move easier towards the substrate holder so that the number of these species incorporated in the growing coating increases. Deposition mechanism is then affected and modification in the composition and the microstructure of the coatings can also occur.

The barrier properties of the coatings depend on their quality; the protection as a function of the immersion time in NaCl solutions increases with the density because of the limitation of voids or pinholes in the coatings. With a 120 W RF bias, the protection is maintained over 8 days. This is a long time with regard to the thickness of the coating (1 μm). Absorption of electrolyte *via* porous defects or pinholes degrades the electric behaviour of coatings and triggers corrosion when electrolyte enters in contact with iron. So, EIS results indicate that plasma-polymerised coatings cannot be used as unique barriers for corrosion protection of steel in aqueous media but their major advantage could be regarded as an improvement of the steel coating adhesive bonding. Further work will be devoted to precisely determining the influence of the pretreatment on the chemical interactions at the plasma-polymerised coating–metal interface and to prove the use of plasma-polymerised coatings as primers.

5. Conclusion

The influence of the RF bias on coatings deposited on iron substrates from a HMDSO–O_2 (80 : 20) precursor mixture has been investigated using gravimetry, SEM, FTIR. The RF bias induces an increase of the deposition rate, a densification of the coatings that become less organic and undergo changes in their morphology. The densification of the coatings enhances the barrier properties.

Acknowledgement

The authors would like to thank Petr Vasina and Mathieu Halbwax for their help in the deposition of the coatings during their stage at the Laboratoire de Physique des Gaz et Plasmas .

References

1 J. H. de Wit, in *Corrosion Mechanisms in Theory and Practice*, ed. P. Marcus and J. Oudar, New York, Basel, Hong Kong, 1995, p. 581.
2 R. L. Twite and G. P. Bierwagen, *Prog. Org. Coat.*, 1998, **33**, 91.
3 J. Marsh, J. D. Scantlebury and S. B. Lyon, *Corros. Sci.*, 2001, **43**, 829.
4 A. Meneguzzi, M. C. Pham, J. C. Lacroix, B. Piro, A. Adenier, C. A. Ferreira and J. C. Lacaze, *J. Electrochem. Soc.*, 2001, **148**(4), B121.
5 T. P. Chou, C. Chandrasekaran, S. J. Limmer, S. Seraji, Y. Wu, M. J. Forbess, C. Nguyen and G. Z. Cao, *J. Non-Cryst. Solids*, 2001, **290**, 153.

6 T. J. Lin, J. A. Antonelli, D. J. Yang, H. K. Yasuda and F. T. Wang, *Prog. Org. Coat.*, 1997, **31**, 351.
7 T. F. Wang, T. J. Lin, D. J. Yang, J. A. Antonelli and H. K. Yasuda, *Prog. Org. Coat.*, 1996, **28**, 291.
8 M. Creatore, F. Palumbo, R. D'Agostino and P. Fayet, *Surf. Coat. Technol.*, 2001, **142–144**, 163.
9 P. Tien, G. Smolinsky and R. Martin, *J. Appl. Opt.*, 1972, **11**, 637.
10 T. Templer, L. Vallier, R. Madar, J. C. Oberlin and R. A. B. Devine, *Thin Solid Films*, 1994, **241**, 251.
11 C. Falcony, A. Ortiz, S. Lopez, J. C. Alonso and S. Muhl, *Thin Solid Films*, 1991, **199**, 269.
12 N. Inagaki, S. Kondo, M. Hirata and H. Urushibata, *J. Appl. Polym. Sci.*, 1989, **30**, 3385.
13 P. Fayet, C. Holland, B. Jaccoud and A. Roulin, *Proceedings of the 38th SVC (Society of Vacuum Coaters) Technical Conference*, 1995, 15.
14 C. Vautrin-Ul, C. Boisse-Laporte, N. Benissad, A. Chausse, P. Leprince and R. Messina, *Prog. Org. Coat.*, 2000, **38**, 9.
15 C. Vautrin-Ul, C. Boisse-Laporte, A. Chausse, P. Leprince and R. Messina, *J. Corrosion Sci. Eng.*, 1999, **2**, paper 3.
16 D. L. Cho and H. Yasuda, *J. Appl. Polym. Sci.: Appl. Polym. Symp.*, 1988, **42**, 233.
17 H. P. Schreiber, M. R. Wertheimer and A. M. Wrobel, *Thin Solid Films*, 1980, **72**, 487.
18 K. D. Conners, W. J. vanOoij, S. J. Clarson and A. Sabata, *J. Appl. Polym. Sci.: Appl.Polym. Symp.*, 1994, **54**, 167.
19 W. J. van Ooij and N. Tang, *Polym. Mater. Sci. Eng.*, 1996, 155.
20 M. Lejeune, O. Durand-Drouhin, J. Henocque, R. Bouzerar, A. Zeinert and M. Benlahsen, *Thin Solid Films*, 2001, **389**, 233.
21 R. Delsol, P. Raynaud, Y. Segui, M. Latreche, L. Agres and L. Mage, *Thin Solid Films*, 1996, **289**, 170.
22 N. Benissad, C. Boisse-Laporte, C. Vallee and A. Groullet, *Surf. Coat. Technol.*, 1999, **820**, 116.
23 M. Moisan and Z. Zakrewski, *J. Phys. D: Appl. Phys.*, 1991, **24**, 1025.
24 J. W. Coburn and M. J. Chen, Optical emission spectroscopy of reactive plasmas. A method for correlating emission intensities to reactive particle density, *J. Appl. Phys.*, 1980, **51**, 3134.
25 R. A. Gottscho and T. A. Miller, Optical techniques in plasma diagnostics, *Pure Appl. Chem.*, 1984, **56**, 189.
26 L. Rolland, M. C. Peignon, Ch. Cardinaud and G. Turban, *Microelectron. Eng.*, 2000, **53**, 375.
27 K. Aumaille, C. Vallée, A. Granier, A. Goullet, F. Gaboriau and G. Turban, *Thin Solid Films*, 2000, **359**, 188.
28 J. Schwarz, M. Schmidt and A. Ohl, *Surf. Coat. Technol.*, 1998, **98**, 859.
29 T. J. Lin, B. H. Chun, H. K. Yasuda, D. J. Yang and J. A. Antonelli, *J. Adhes. Sci. Technol.*, 1991, **5**(10), 893.
30 N. Benissad, K. Aumaille, A. Granier and A. Goullet, *Thin Solid Films*, 2001, **384**, 230.
31 R. A. B. Devine, *J. Vac. Sci. Technol., A*, 1988, **6**, 3154.
32 H. K. Yasuda, T. F. Wang, D. L. Cho, T. J. Lin and J. A. Antonelli, *Prog. Org. Coat.*, 1997, **30**, 31.
33 J. M. McIntyre and H. Q. Pham, *Prog. Org. Coat.*, 1996, **27**, 201.
34 W. J. Van Ooij and K. D. Conners, *Polym. Mater. Sci. Eng.*, 1996, 153.
35 F. Mansfeld, *Corrosion*, 1981, **36**, 301.
36 M. Stratmann, R. Freser and A. Leng, *Electrochim. Acta*, 1994, **39**, 1207.
37 P. Raynaud, T. Amilis and Y. Segui, *Appl. Surf. Sci.*, 1999, **138–139**, 285.
38 F. Nicolazo, A. Goullet, A. Granier, C. Vallée, G. Turban and B. Grolleau, *Surf. Coat. Technol.*, 1998, **98**, 1578.
39 P. Favia, R. d'Agostino and F. Fracassi, *Pure Appl. Chem.*, 1994, **66**, 1373.
40 N. Shirtcliffe, P. Thiemann, M. Stratmann and G. Grundmeier, *Surf. Coat. Technol.*, 2001, **142–144**, 1121.